express
polymer letters

*Research article*

# Achieve balanced stiffness and toughness properties of nanocomposites based on poly(lactic acid)/polyolefin by using fuzzy rule-based system

*Sajjad Daneshpayeh[1]* , *Ismail Ghasemi[2]\** , *Faramarz Ashenai Ghasemi[1]* ,
*Valiollah Panahizadeh[1]*

[1]Faculty of Mechanical Engineering, Shahid Rajaee Teacher Training University, Shabanlou, 16788-15811 Tehran, Iran
[2]Department of Polymer Engineering, Iran Polymer and Petrochemical Institute (IPPI), Research Blvd, 14977-13115 Tehran, Iran

**Abstract.** Using filler and impact modifiers for balancing stiffness and toughness properties is a common strategy for modification of polymer matrices' performance. Nanocomposites based on poly lactic acid/polyolefin elastomer/including multi-walled carbon nanotubes/carbon black nanoparticles (PLA/POE/MWCNTs/CB) were produced using an internal mixer. Fuzzy rule- based system (FRBS) was applied to predict and simulate of mechanical properties of the samples. The field-emission scanning electron microscopy (FESEM) was applied to determine the state of nanofillers distribution. The FESEM images showed that the carbon black and MWCNTs individually were well distributed. But, the simultaneous addition of nanofillers by more than 1 wt% from each one led to their agglomeration. The results illustrated that the presence of MWCNTs and carbon black separately and simultaneously led to an increase in tensile strength and Young's modulus. The simultaneous presence of them led to an improvement in impact strength by 30%. Also, by incorporating POE into the PLA matrix, a significant increment in impact strength was obtained by 110%. The obtained surface plots from FRBS revealed that there is an interaction between nanofillers effects on the mechanical properties. Finally, a good agreement between the predicted mechanical properties using FRBS and evaluation tests led to extract accurate models with proper $R^2$ and standard error for all responses.

**Keywords:** biodegradable polymers, poly(lactic acid), nanocomposites, mechanical properties, fuzzy logic

## 1. Introduction

Poly lactic acid (PLA) is obtained from renewable materials such as beets and corn. This biocompatible thermoplastic shows better mechanical properties compared to general-purpose petroleum-derived polymers [1]. PLA can be a good candidate for use in the packaging of food products, medicine, electrical tools, and automotive industries. PLA is a brittle polymer with low impact strength and elongation at break [2, 3]. Many efforts have been made to improve the PLA properties. Copolymerization, blending, and incorporation of fillers are well-known methods for modification of PLA performance [4–6].

To improve impact strength and toughness, the brittle polymers are usually blended with polymeric materials with elastomeric properties [7]; such as polyethylene (PE) [8], ethylene-propylene-diene monomer (EPDM) [9], poly butylene adipate-*co*-terephthalate (PBAT) [10], Polyolefin elastomers (POEs) [11] and so on. Many efforts have been made to improve the impact properties of PLA. For example, adding 4 wt% of polyurethane to PLA leads to a significant

---

*Corresponding author, e-mail: i.ghasemi@ippi.ac.ir

increase in its impact strength from 11 to 80 J/m and a reduction in its tensile strength by 2%. [12]. It was found that the addition of thermoplastic polyurethane elastomer (TPU) to PLA improves its elongation at break and impact strength but decreases its strength and modulus significantly [13].

Recently, toughening of brittle polymers by POE has been considered because of its superior elasticity and toughness. Using POE as an impact modifier in polypropylene and polyamide has been reported [7]. Zhou *et al*. [11] reported that adding POE up to 20 wt% was associated with 71% increase in PLA impact strength. Interestingly, the presence of 5 wt% of POE not only did not reduce the tensile strength of the PLA but also improved it by 7%. Also, Yang *et al*. [14] showed that the presence of 20 wt% POE into Polybutylene terephthalate matrix led to an increase in its impact strength by 37%, whereas the tensile strength decreases only slightly. The results of Guo *et al*.'s work [15] show that adding 20 wt% POE to the polystyrene matrix significantly increases its impact strength by 266%. By comparing the performance of POE and other impact modifiers in the different matrices, one can find that POE can reduce the brittleness significantly and does not show a severe reduction effect on stiffness [16].

The incorporation of nanomaterials as a third component to balance between toughness and stiffness of the compound has been reported in the literature [17, 18]. Nanomaterial with different shapes including MWCNTs [19, 20], graphene nanoplatelets [21], graphene oxide [22], carbon black [23], titanium dioxide [24], nano clay [25] and silica [26] have used in PLA matrix. da Silva *et al*. [17] examined the modulus and elongation at break of PLA/PE/TiO$_2$ nanocomposites and showed that the addition of TiO$_2$ nanoparticles to the PLA/PE matrix increased the modulus from 817 to 1490 MPa and reduced the elongation at break from 1.9 to 1.1%. Chieng *et al*. [18] concluded that the addition of graphene nanoplatelets up to 1 wt% to the PLA/PEG binary matrix was associated with an increase in tensile strength (from 22 to 30 MPa), Young's modulus (from 420 to 780 MPa), and elongation at break (from 400 to 500%).

Simultaneous addition of nanofillers to a polymer matrix and the fabrication of polymer hybrid nanocomposites has led to the achievement of a balance among mechanical properties [27]. The hybrid nanocomposites properties are exclusively related to factors like matrix, type of nanofillers and their dimensions, nanofillers shape, and fillers-matrix adhesion [28]. The mechanical and thermal properties of PLA/ TPU/nano silica/ nano clay hybrid nanocomposites were studied by Palawat *et al*. [29]. Their results showed that the simultaneous presence of 2 wt% nanoclay and 3 wt% nano SiO$_2$ into PLA/PU binary matrix led to an increase in elastic modulus by 16%. In addition, impact strength and elongation at break were reduced slightly.

The fuzzy rule- based systems (FRBSs) method has been used for various purposes, such as modeling the mechanical properties of concrete [30], mechanical properties of polymeric nanocomposites [31], and optimizing the different parameters in different fields [32]. FRBSs method reduces the number of tests that must be carried out, which saves time and money. In addition, this method is able to recognize the effect of the simultaneous presence of two input parameters on a response with the help of surfaces. The particular advantage of the FRBSs method over other methods is its rules section. In this section, many outputs can be obtained by changing the input variables in the defined domain. This leads to extract an accurate regression model [33].

This work is motivated by current researches in the field of balancing between toughness and stiffness of PLA using nanofillers and impact modifiers. The main goal of this work is to investigate of the effect of hybrid nanofiller instead of one filler in the compound. A fuzzy rule- based systems method was used to predict and model the mechanical properties of nanocomposites based on PLA/POE/MWCNTs/ Carbon black. Nanocomposites samples including MWCNTs (at 0–3 wt%), carbon black (at 0–3 wt%), and POE (at 0–20 wt%) were made by an internal mixer. The effect of hybrid systems on mechanical properties, including the tensile and impact strength and Young's modulus, were studied using FRBS method.

## 2. Experimental
### 2.1. Materials
Poly(lactic acid) (05 BIOKAS based grades) employed in this work with density 1.25 g/cm$^3$, melt flow index 7 g/10 min (210 °C/2.16 kg), tensile strength 45 MPa, elongation at break 3% and impact strength 4 J/m was provided from CHEMIE KAS GmbH, Vienna, Austria; Polyolefin elastomer (Tafmer DF640) with melt flow index of 3.6 g/10 min (190 °C/ 2.16 kg,), tensile strength 3 MPa purchased from

Mitsui Chemicals, Tokyo, Japan; Multi-walled carbon nanotubes with 25 nm diameter, 10 μm length and 220 m$^2$/g specific surface area were provided from united nanotech, Karnataka, India. Carbon black with density0.38 g/ml and nano-size of 50 nm were prepared from US-nano, Houston, TX USA.

## 2.2. Sample preparation

The materials were blended by melt-blending using a Haake internal mixer type HBI SYS 90 (Thermo Fisher Scientific Company, Loughborough, United Kingdom) at 60 rpm and 180 °C for 10 min. First, the polymeric materials were mixed for 3 minutes until they melted and formed a polymer alloy, then the nanofillers were added to the mixing chamber for 7 minutes. The samples were formed into sheets with 3mm thickness at 190 °C by hot-press molding with square steel mold (200×200 mm$^2$) under 50 MPa pressure. Finally, the samples for tensile and impact tests under D638 type IV (with 9.53×63.5×3 mm$^3$ dimensions) and D256 (with 63×12.7×3 mm$^3$ dimensions) standards from the sheets were prepared by a special punch. The samples were produced in 30 different modes, as shown in Table 1.

Five sample replications were considered for testing each compound.

## 2.3. Characterization

RESIL IMPACTOR instrument (Torino, Italy) was used to perform the Izod notch method impact testing at room temperature according to ASTM D256. The energy obtained from the impact test for each sample was divided on the width of the sample, and thus, the impact energy of each sample was extracted in terms of J/m. Zwick/Roell–Z100 instrument (Fürstenfeld, Germany) also was used to carry out the tensile test according to ASTM D638 with a crosshead speed of 5 mm/min at room temperature. The output of the Zwick/Roell–Z100 instrument provided a stress-strain diagram and a PDF file including T-strength, Young's modulus, and deformation at break for each sample tested. In addition, the average of the three runs was reported for impact and final tensile results. To observe the quality dispersion of nanofillers in the polymer field, VEGA TESCAN FESEM (Kohoutovice, Czech Republic) with voltage 20 kV, in a vacuum was used. Before extracting the FESEM images, the surfaces of the samples were coated with gold.

**Table 1.** Blend samples states.

| Sample No. | PLA [wt%] | POE [wt%] | MWCNTs [wt%] | Carbon black [wt%] |
|---|---|---|---|---|
| 1 | 100 | 0 | 0 | 0 |
| 2 | 90 | 10 | 0 | 0 |
| 3 | 80 | 20 | 0 | 0 |
| 4 | 99 | 0 | 1 | 0 |
| 5 | 98 | 0 | 2 | 0 |
| 6 | 97 | 0 | 3 | 0 |
| 7 | 89 | 10 | 1 | 0 |
| 8 | 88 | 10 | 2 | 0 |
| 9 | 87 | 10 | 3 | 0 |
| 10 | 79 | 20 | 1 | 0 |
| 11 | 78 | 20 | 2 | 0 |
| 12 | 77 | 20 | 3 | 0 |
| 13 | 99 | 0 | 0 | 1 |
| 14 | 98 | 0 | 0 | 2 |
| 15 | 97 | 0 | 0 | 3 |
| 16 | 89 | 10 | 0 | 1 |
| 17 | 88 | 10 | 0 | 2 |
| 18 | 87 | 10 | 0 | 3 |
| 19 | 79 | 20 | 0 | 1 |
| 20 | 78 | 20 | 0 | 2 |
| 21 | 77 | 20 | 0 | 3 |
| 22 | 99 | 0 | 0.5 | 0.5 |
| 23 | 98 | 0 | 1 | 1 |
| 24 | 97 | 0 | 1.5 | 1.5 |
| 25 | 89 | 10 | 0.5 | 0.5 |
| 26 | 88 | 10 | 1 | 1 |
| 27 | 87 | 10 | 1.5 | 1.5 |
| 28 | 79 | 20 | 0.5 | 0.5 |
| 29 | 78 | 20 | 1 | 1 |
| 30 | 77 | 20 | 1.5 | 1.5 |

## 2.4. Fuzzy inference system

Fuzzy inference is a method that interprets the values in the input vector and, based on some sets of rules, assigns values to the output vector. Fuzzy inference is the process of formulating the mapping from a given input to an output using fuzzy logic. The mapping provides a basis from which decisions can be made or patterns discerned. The fuzzy inference procedure requires membership functions, fuzzy logic operators, and if-then rules [34].

Two main types of fuzzy inference systems can be implemented: Mamdani-type and Sugeno-type. In both Mamdani and Sugeno types, the membership function must be defined for the input and output variables at first. Then, the If-Then rules must be written based on defined inputs and outputs functions. Mamdani-type and Sugeno-type fuzzy inferences

have the main difference, so that, for the Sugeno-type fuzzy inference, the output membership functions are only linear or constant [33, 35]. We used the Sugno-type because the outputs in this study are the results of mechanical tests and constant values. The input parameters, namely POE, MWCNTs, and carbon black, were considered at different levels (each nanofiller at four and POE at three levels) are given in Table 2.

Membership functions for input variables are shown in Figure 1. The Gaussian membership functions were determined in the range of 0–3 wt% for nanofillers and 0–20 wt% for POE, respectively. Gaussian membership functions have been used for several reasons;

– Local, although not strictly compact,

**Table 2.** The range of input variables.

| Input parameters | Levels use [wt%] | | | | | |
|---|---|---|---|---|---|---|
| MWCNTs | 0 | 0.5 | 1 | 1.5 | 2 | 3 |
| carbon black | 0 | 0.5 | 1 | 1.5 | 2 | 3 |
| POE | 0 | 10 | 20 | – | – | – |



a)



b)



c)
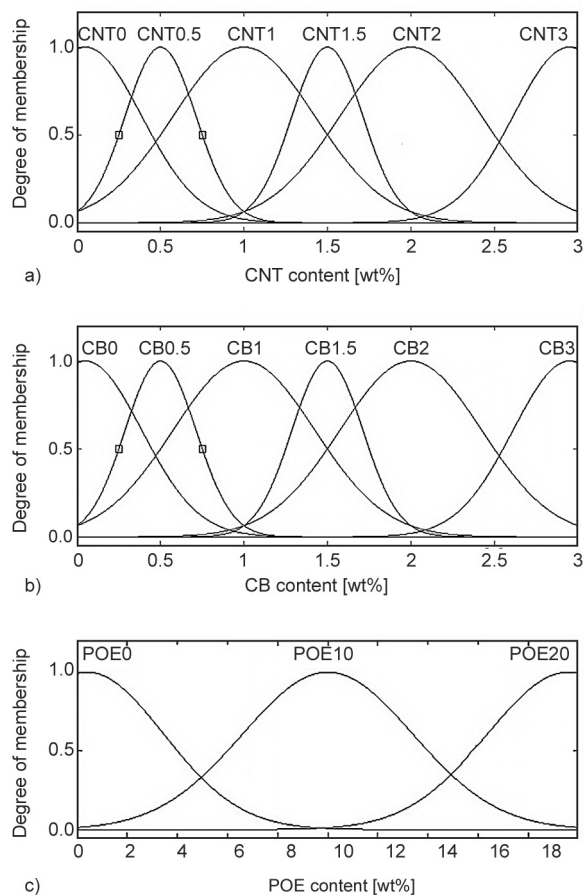
**Figure 1.** Membership function plots for inputs: a) MWCNTs, b) carbon black nanoparticles and c) POE.

– The output is very smooth
– And not a probability.
Also, Gaussian fuzzy membership functions are quite popular in the fuzzy logic literature, as they are the basis for the connection between fuzzy systems and radial basis function (RBF) neural networks.

As shown in Figure 1a and 1b, six input membership functions are determined based on the number of levels specified for each nanofiller. In addition, three input membership functions are defined for the POE (Figure 1c).

In the following, the fuzzy rules must be written. If-Then rule statements are used to formulate the conditional statements that comprise fuzzy logic. A single fuzzy If-Then rule assumes the form:

If **x** is *A* Then **y** is *B*

where *A* and *B* are variables defined by fuzzy sets on the ranges (*i.e.*, the universe of discourse) *X* and *Y*, respectively. The If-part of the rule '**x** is *A*' is called the antecedent or premise, and the Then-part of the rule '**y** is *B*' is called the consequent. According to Table 1 and based on 30 combined states, 30 rules are written for mechanical properties the form:

If (POE is *A* and MWCNTs is *B* and carbon black is *C*) Then (tensile strength is *X* and *Y*oung's modulus is *Y* and impact strength is *Z*)

where *A*, *B*, and *C* represent the values of the input variables (POE, MWCNTs, and carbon black) according to Table 2, and the *X*, *Y*, and *Z* illustrate the results of the tested mechanical properties based on *A*, *B*, and *C* values.

## 3. Results and discussion
### 3.1. Morphology

It is useful to start with an explanation of the morphology. It is well known that interfacial interaction between the nanofillers and polymer matrix is an important factor affecting the mechanical properties of polymer nanocomposites. In other words, suitable mechanical properties are obtained when the nanofillers (with a high aspect ratio and surface area) are well dispersed in the polymer matrix [36, 37]. The morphologies of polymer nanocomposites are highly controlled by the interactions between polymer matrix and nanofillers.

Figure 2, show the FESEM micrographs of the nanocomposites samples containing 1, 2, and 3 wt% of MWCNTs with three different magnifications

(1000×, 5000×, and 15 000×) at constant 10 wt% POE content.

As expected, a droplet-matrix morphology of PLA/POE has been formed, and POE particles have dispersed in PLA matrix and improve the toughness because of its lower modulus through the well-known

mechanisms such as shear banding cavitation and multi crazing [38]. On the other hand, MWCNTs are clearly exhibited as a tubular shape and a similar structure observed in all nanocomposites systems. According to the various parts of Figure 2, MWCNTs on all three levels are well dispersed in the polymeric
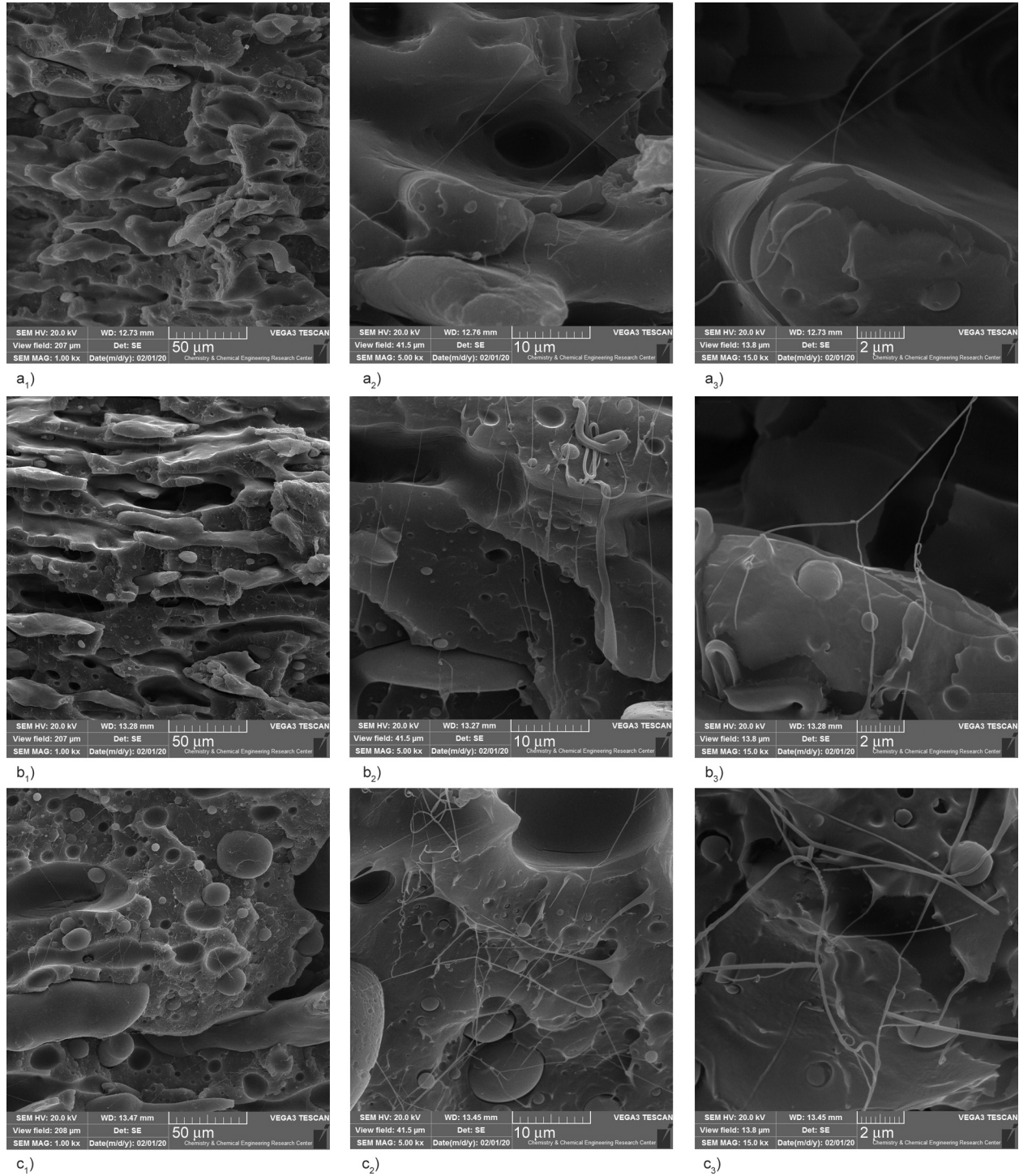


**Figure 2.** FESEM images at three different magnifications for: a) sample with 10 wt% POE and 1 wt% MWCNTs ($a_1$ with 1000× magnification, $a_2$ with 5000× magnification and $a_3$ with 15 000× magnification), b) sample with 10 wt% POE and 2 wt% MWCNTs ($b_1$ with 1000× magnification, $b_2$ with 5000× magnification and $b_3$ with 15 000× magnification), and c) sample with 10 wt% POE and 3 wt% MWCNTs ($c_1$ with 1000× magnification, $c_2$ with 5000× magnification and $c_3$ with 15 000× magnification).

matrix, and no agglomeration or clumping is observed.

Also, the MWCNTs show reasonable dispersion in random orientations among the polymeric matrix for different loadings. It can be said that the MWCNTs not only did not pulled out of the samples after they were broken but also were embedded in the matrix and stick to it [19]. Fabrication of nanocomposites containing MWCNTs in the range of 0 to 3 wt% by internal mixer has led to their proper mixing in the matrix. Proper dispersion of MWCNTs has resulted in good filler-matrix interactions. This allows the nanotubes to fit snugly into the matrix and adhere to it as well. Proper adhesion, wetting, and filler-matrix interaction are well observed in the Figure 2a$_2$, 2a$_3$, 2b$_2$ and 2c$_2$.

FESEM images of samples from surface broken sections of nanocomposites samples including carbon black nanoparticles different loading in the three magnifications (1000×, 5000×, and 10 000×) at constant 10 wt% POE content are depicted in Figure 3. Similar to previous samples, a droplet-matrix morphology is observed from PLA/POE blend. As can be seen from different parts of Figure 3a and 3b, the presence of carbon black nanoparticles at two levels of 1 and 2 wt% have a good and uniform distribution in the PLA/PEO matrix. On the other hand, at 3 wt% loadings (Figure 3c) of these nanofillers, the particles are stuck together, and agglomeration has occurred. The location of the agglomeration of the particles in the 3 wt% loadings are shown in Figure 3c$_2$ and 3c$_3$ by white arrows. Figure 3c$_2$ shows that by increasing the amount of carbon black nanoparticles up to 3 wt%, there are no proper filler-matrix interactions, and the nanoparticles have a severe tendency to accumulate due to the existence of oxygen-containing groups on their surface. The poor dispersion and aggregation of carbon black nanoparticles may lead to the poor mechanical performance of nanocomposites.

FESEM images of the simultaneous presence of MWCNTs and carbon black nanoparticles in the PLA/10 wt% POE matrix are shown in Figure 4. The mechanical properties of these samples may be affected by filler-filler and filler-matrix interactions. Figure 4a shows the dispersion of the sample with 0.5 wt% MWCNTs/0.5 wt% carbon black nanoparticles with three different magnifications 1000×, 15 000×, and 35 000×. It seems there is no considerable interaction between two fillers at the contents

of the nanoparticles, and the simultaneous presence of them in the matrix has been associated with good distribution.

In Figure 4b, the simultaneous presence of 1 wt% MWCNTs/1 wt% carbon black nanoparticles in the matrix are observed. The dispersion of both of the nanofillers, in this case, is also almost appropriate and acceptable. Nanotubes with good dispersion and short lengths are still visible in Figure 4b$_2$ and 4b$_3$. On the other hand, Figure 4b$_3$ with larger magnification shows that carbon black nanoparticles and MWCNTs with short lengths have started to stick together. The interlocking parts of both nanofillers can be seen in Figure 4b$_3$ with the help of an arrow. Interlocking parts form a more uniform reinforcing phase which leads to better mechanical performances. It seems the empty spaces between MWCNTs are filled by carbon black particles and a mechanical percolation threshold has been created at these conditions.

In addition, some severe aggregations are detectable in the sample, including 1.5 wt% MWCNTs/1.5 wt% carbon black nanoparticles (Figure 4c). The simultaneous presence of 1.5 wt% of each of the nanofillers has created two types of agglomerations. One agglomeration is related to the separate aggregation of each of them, and the other type of agglomeration is related to the sticking of two nanofillers to each other.

Accumulation of carbon black nanoparticles and the adhesion of both nanofillers are illustrated in Figure 4c$_3$ using arrows and circles, respectively. Due to the intense accumulation of nanofillers in the matrix, it is expected that these aggregations act as impurities and porosity in different places of the matrix and reduce the mechanical properties of the structure. The distribution of nanofillers in polymeric phases is also important in the toughness and stiffness of the samples. The location of nanofillers is balanced by the thermodynamic affinity of the components and kinetic of nanofillers' migration between two polymeric phases, which is influenced by mixing time. Selective distribution using surface treatment of nanofiller is a well-known strategy for modification of morphology [39, 40]. In this study, it seems due to the matching of fillers and POE structures, the existence of nanofillers in POE is more probable. In this case, POE phase shows more elasticity and causes to forming finer dispersed phase and more toughness.
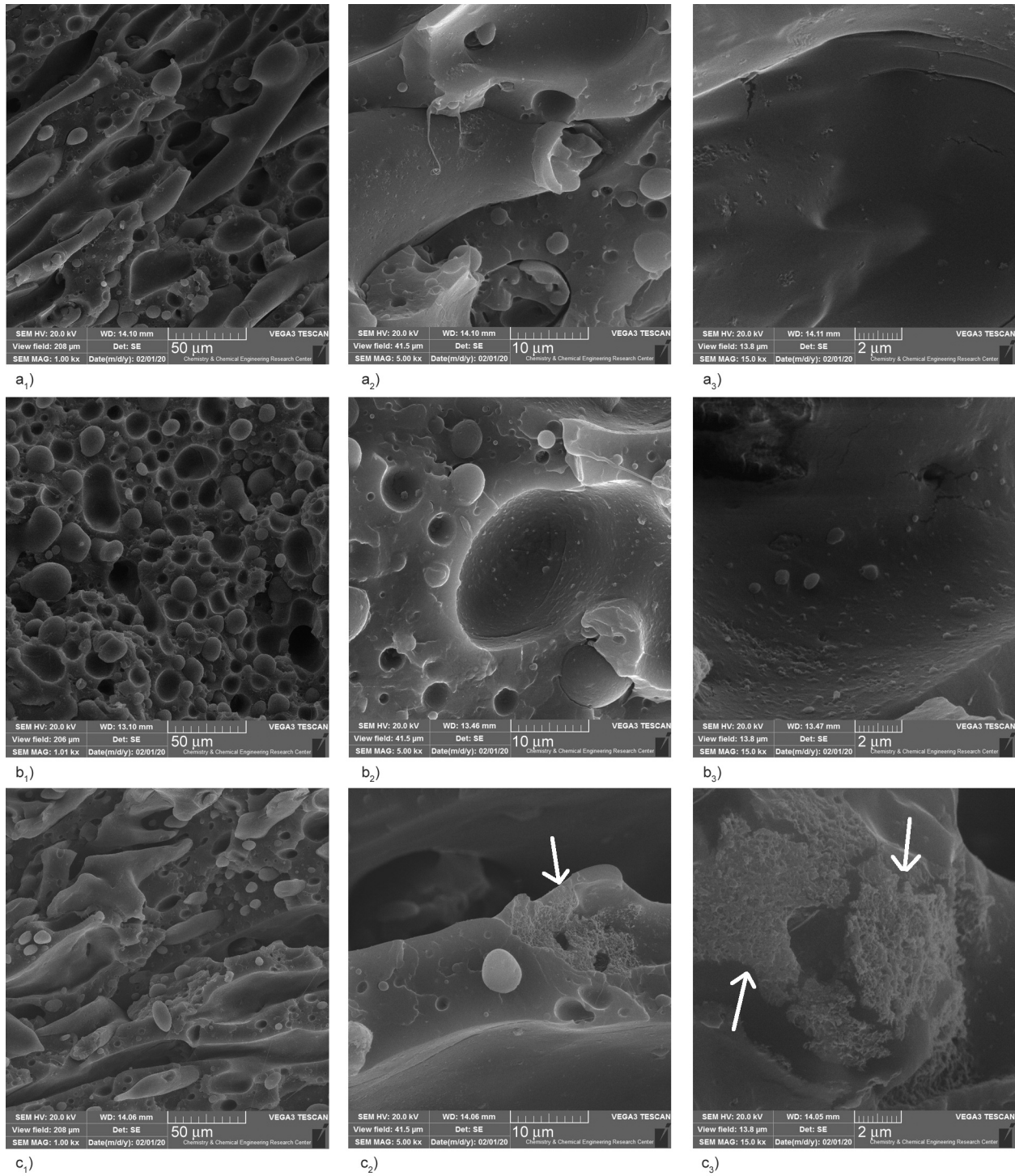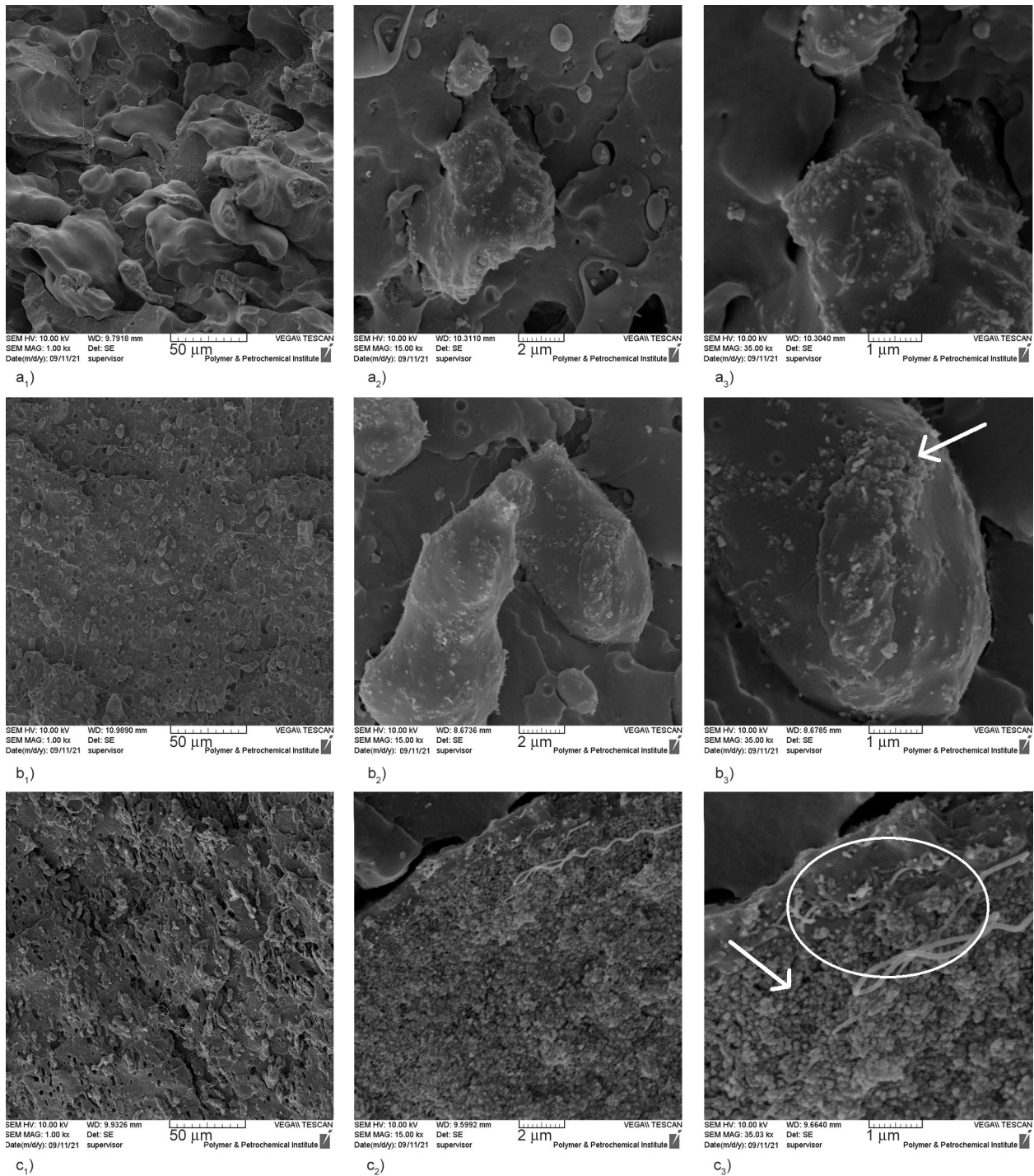
**Figure 3.** FESEM images for: a) sample with 10 wt% POE and 1 wt% carbon black ($a_1$ with 1000× magnification, $a_2$ with 5000× magnification and $a_3$ with 15 000× magnification), b) sample with 10 wt% POE and 2 wt% carbon black ($b_1$ with 1000× magnification, $b_2$ with 5000× magnification and $b_3$ with 15 000× magnification), and c) sample with 10 wt% POE and 3 wt% carbon black ($c_1$ with 1000× magnification, $c_2$ with 5000× magnification, and $c_3$ with 15 000× magnification).

## 3.2. Fuzzy model prediction

By using the rules section of FRBSs one can change the input variables in the defined range, and new output values for responses can be obtained. Since the results obtained from the rules section are only predictions and not certain, the system has to

be evaluated and verified by performing validation tests. The validation tests were carried out to verify the feasibility and reproducibility of the FRBSs method adopted in this work. To evaluate the system for tensile strength, Young's modulus, and impact strength, two new hybrid nanocomposites were

**Figure 4.** FESEM images for: a) sample with 10 wt% POE and 0.5 wt% carbon black/0.5 wt% MWCNTs ($a_1$ with 1000× magnification, $a_2$ with 15 000× magnification and $a_3$ with 35 000× magnification), b) sample 10 wt% POE and 1 wt% carbon black/1 wt% MWCNTs ($b_1$ with 1000× magnification, $b_2$ with 15 000× magnification and $b_3$ with 35 000× magnification), and c)sample 10 wt% POE and 1.5 wt% carbon black/1.5 wt% MWCNTs ($c_1$ with 1000× magnification, $c_2$ with 15 000× magnification and $c_3$ with 35 000× magnification).

made, and tensile and impact tests were performed. The details of the selected input variable values, the results of the FRBSs predictions, and the results of confirmation tests for the mechanical properties are presented in Table 3.

As can be seen from Table 3, the results of the validation tests are in good agreement with the predicted results using the FRBSs method, which means the predicted outputs of this method are reliable for mechanical properties.

An accurate model could be obtained when enough data are used. After confirming the reliability of the results predicted by the FRBSs by performing validation tests for each mechanical property, the

**Table 3.** Results of confirmation experiments and prediction values for mechanical properties.

| Selected compounds | Tensile strength | | |
|---|---|---|---|
| | Confirmation experiment [MPa] | Prediction [MPa] | Error [%] |
| 10 wt% POE/1 wt% MWCNTs/2 wt% carbon black | 42.65 | 39.5 | 8 |
| 10 wt% POE/2 wt% MWCNTs/1 wt% carbon black | 40.00 | 37.4 | 7 |
| | Young's modulus | | |
| | Confirmation experiment [MPa] | Prediction [MPa] | Error [%] |
| 10 wt% POE/1 wt% MWCNTs/2 wt% carbon black | 371 | 344 | 8 |
| 10 wt% POE/2 wt% MWCNTs/1 wt% carbon black | 337 | 344 | 2 |
| | Impact strength | | |
| | Confirmation experiment [J/m] | Prediction [J/m] | Error [%] |
| 10 wt% POE/1 wt% MWCNTs/2 wt% carbon black | 9.38 | 8.23 | 14 |
| 10 wt% POE/2 wt% MWCNTs/1 wt% carbon black | 7.78 | 8.28 | 6 |

contents of input variables, including two nanofillers and POE, were changed 441 times in the defined range. Therefore, 441 outputs were obtained for each mechanical property. In the following, with the help of a large number of available inputs and outputs, third-degree regression models for mechanical properties with three variables (POE, MWCNTs, and carbon black) were extracted by Microsoft Excel Office Software. The results of deriving regression models for tensile strength, Young's modulus, and impact strength are presented in Table 4.

One measure of goodness of fit for presented regression models is the $R^2$ (coefficient of determination), which in ordinary least squares with an intercept ranges between 0 and 100%. As can be seen from Table 4, the range achieved $R^2$ for presented models for tensile strength is above 80%, and for impact strength and Young's modulus are above 90%. These results for $R^2$ indicate a good fitting of the experimental

data. One problem in the case of $R^2$ as a measure of model validity is that it can always be increased by adding the number of input and output variables. However, the $R^2$ close to 100% does not guarantee the fitting of the model and the data well. Therefore, other factors should be considered to determine the validity of the models [41, 42].

The standard error of the regression has several advantages. Standard error indicates that how far the data points are from the regression line on average. The standard error must have lower values because it signifies that the distances between the data points and the fitted values are small. The standard error is also valid for both linear and nonlinear regression models. This fact is convenient if you need to compare the fit between both types of models [43].

According to Table 4, the standard error only for the presented model for Young's modulus is higher than 3. It can be concluded that $R^2$ and standard error values

**Table 4.** Regression models for mechanical properties in terms of POE, MWCNTs, and carbon black contents.

| Regression model | $R^2$ [%] | Standard error |
|---|---|---|
| T-strength (POE, MWCNTs, carbon black) $= 43.802 + 11.399x - 7.973x^2 + 1.651x^3 + 14.310y - 4.292y^2 + 0.042y^3 - 1.833z + 0.070z^2 + {} + 1.464yx^2 - 6.226xy - 0.069xz - 0.186yz + 0.052xyz - 0.212xy^3 + 1.792xy^2 - 0.274yx^3$ | 81 | 2.91 |
| Y-modulus (POE, MWCNTs, carbon black) $= 304.655 + 52.196x - 15.646x^2 + 4.190x^3 + 96.020y - 6.198y^2 - 4.779y^3 - 4.246z - 0.018xz^2 + {} + 20.297yx^2 - 77.446xy - 0.094xz - 0.672yz + 0.216xyz - 1.925xy^3 + 17.431xy^2 - 3.562yx^3$ | 91 | 13.27 |
| Impact (POE, MWCNTs, carbon black) $= 5.712 - 0.816x + 0.203x^2 - 0.052x^3 + 1.466y - 1.104y^2 + 0.188y^3 + 0.312z - 0.002z^2 + 0.262xy + {} + 0.005xz - 0.014yz - 0.029yx^2 + 0.004xy^3 + 0.017yx^3 - 0.040x^2y^2 + 0.010x^2y^3$ | 92 | 0.48 |

MWCNT = $x$,
CB = $y$ and
POE = $z$

show that almost all the models presented using the FRBSs method are reliable for the mechanical properties of PLA/POE/ nanofillers nanocomposites.

## 3.3. Mechanical properties
### 3.3.1. Tensile strength
The effect of input variables content, including POE and nanofillers, on the tensile strength of the PLA matrix, is shown in Figure 5. As seen in Figure 5a, tensile strength continually increases with the addition of MWCNTs content from 38 to 52 MPa, an increase by 37%. As mention earlier in Figure 2, adding MWCNTs in all levels was associated with proper dispersion into the matrix. In other words, increment of tensile strength may be attributed to good filler-matrix interactions and the proper mixing of MWCNTs with high surface area and aspect ratio [44]. Similar results have been reported by other

researchers who studied on PLA/MWCNTs nanocomposites [19, 20].
Figure 5b indicates that adding carbon black nanoparticles up to 2 wt% was able to create a significant increase in tensile strength of the PLA 67 MPa, which is 76% higher than of the pure PLA. This remarkable improvement in tensile strength can also be related to the proper mixing of nanoparticles in the matrix [45]. Further addition of carbon black content up to 3 wt% decreased of tensile strength to 40 MPa, only slightly higher than of pristine PLA. This phenomenon is influenced by the agglomeration of carbo black that was visible in Figure 3c.
The tensile strength of PLA/MWCNTs/carbon black hybrid nanocomposites samples is exhibited in Figure 5c. From Figure 5c, tensile strength illustrates enhancing trend from 38 to 59 MPa with the simultaneous increase of MWCNTs and carbon black
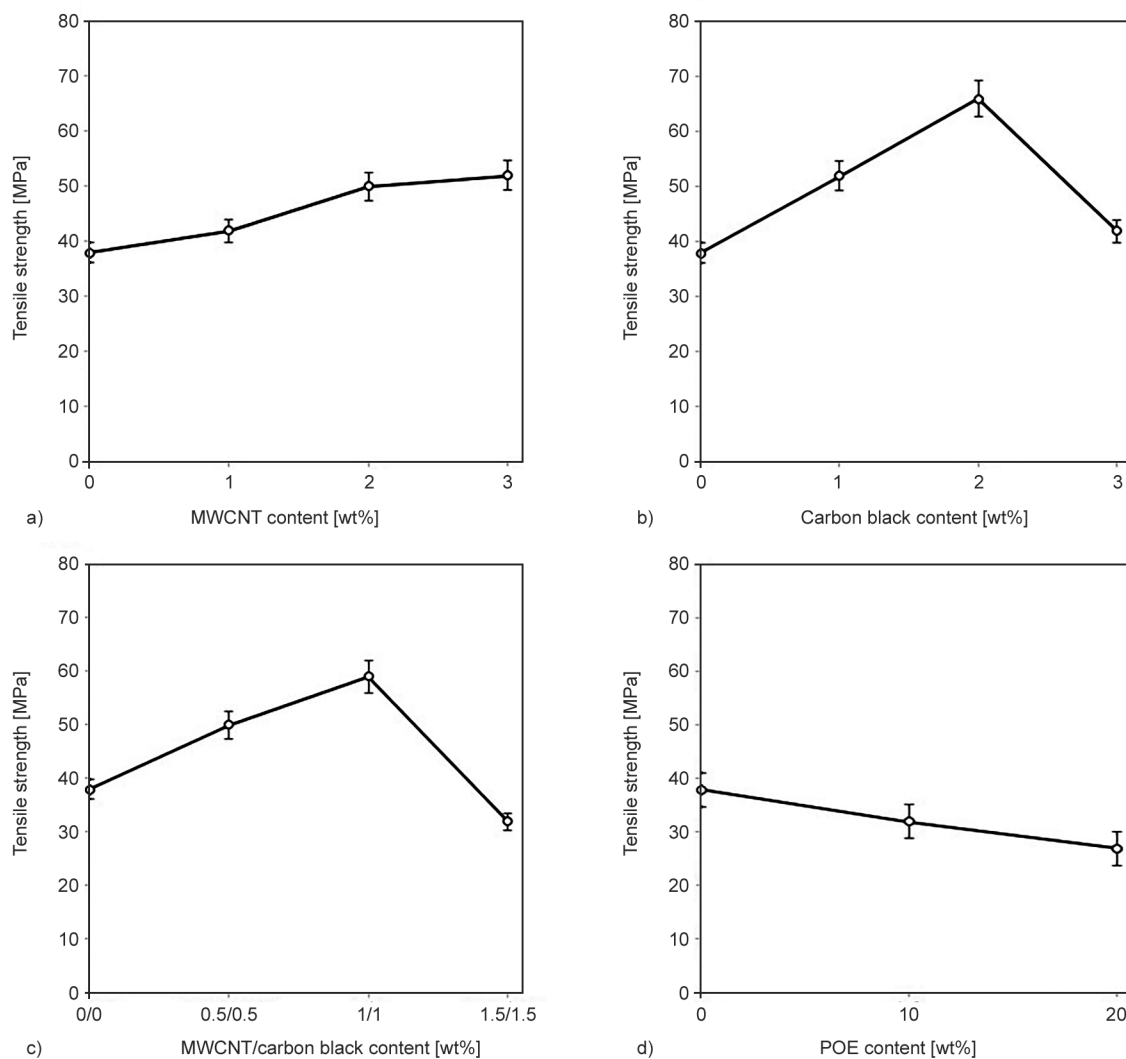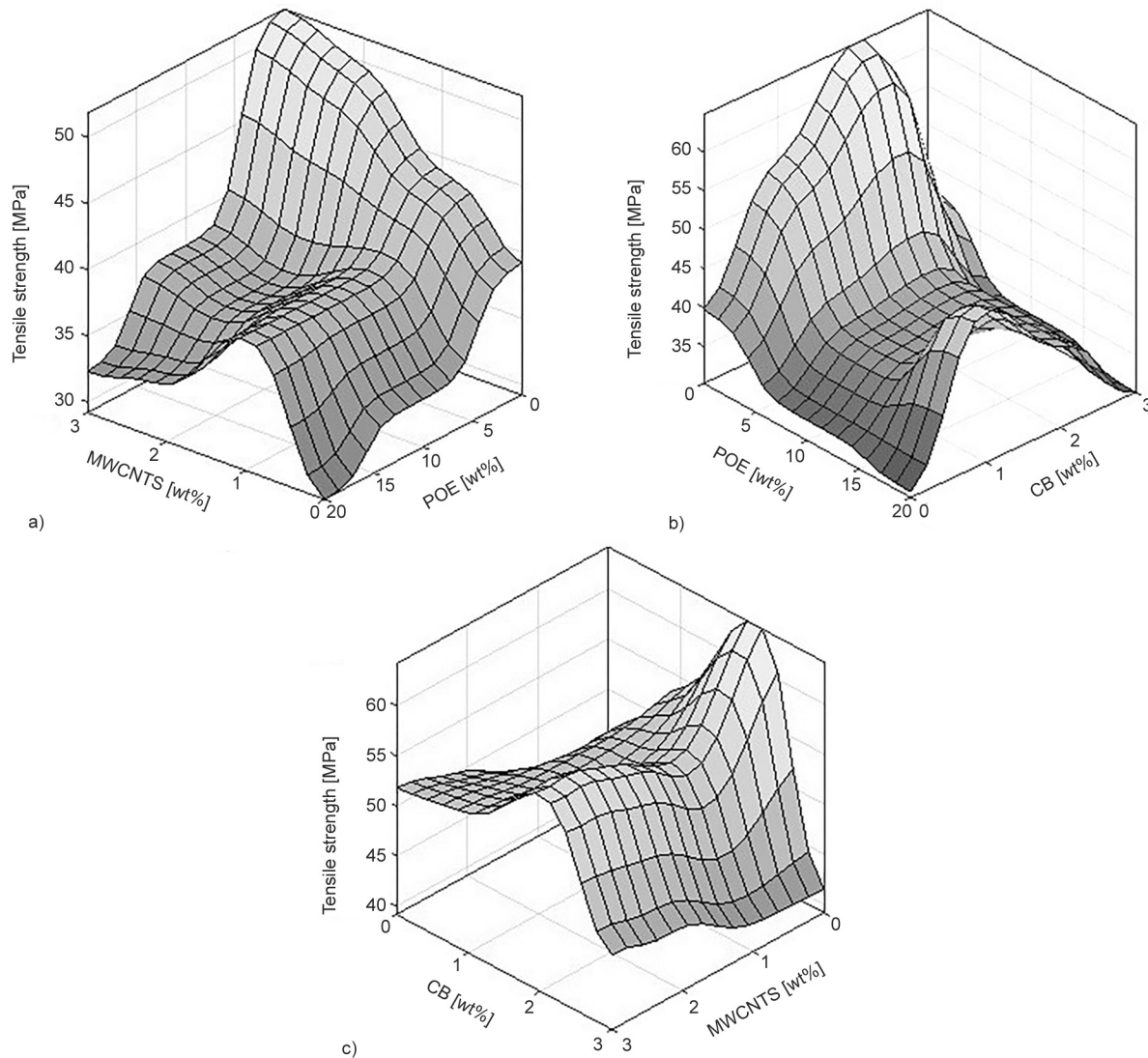


**Figure 5.** Tensile strength of PLA *versus*: a) MWCNTs, b) carbon black, c) MWCNTs/carbon black, and d) POE content.

up to 1 wt% content of each one. Based on the good dispersion of nanofillers in the hybrid state (as shown in Figure 4a and 4b), it was expected that this enhancing trend has occurred in the case of the tensile strength of nanocomposites. Efficient filling of free spaces between MWCNTs by carbon black nanoparticles can be imagined in these samples. Further, increase in both nanofillers by 1.5 wt% content of each one because of severe aggregation is declined the tensile strength of PLA matrix. This severe aggregation was indicated in the morphology analysis (Figure 4c). According to Figure 5d, an increase in POE content from low (0 wt%) to high (20 wt%) loadings caused a declining trend in the tensile strength of the PLA matrix. When the up to 5 wt% content of POE increase in the PLA matrix, the crystallinity of PLA reduces, and decreasing the crystallinity is accompanied

by reducing in tensile strength [11]. Similar results in the case of tensile strength of PLA/POE blends were also achieved by Forghani *et al.* [46]. With respect to different parts of the Figure 5, it is demonstrated that the highest value of tensile strength was obtained by the addition of 2 wt% content of carbon black into the PLA matrix by 67 MPa. On the other hand, the lowest value of tensile strength was obtained by the addition of 1.5 wt%/1.5 wt% of MW-CNTs/carbon black by 29 MPa.

The surfaces extracted from the FRBSs method for tensile strength are presented in Figure 6. With the help of these surfaces, it is possible to see how two input variables simultaneously affect each of the output response. It can also be detected if there is an interaction between two input factors affecting a response.



**Figure 6.** Surface plots for tensile strength of PLA matrix versus: a) POE and MWCNTs, b) POE and carbon black, and c) MWCNTs and carbon black.

As can be seen from Figure 6a, the addition of MWCNTs shows two different behavior in the presence of different POE loadings. From Figure 6a, it is observed that Young's modulus considerably increased with increasing the amount of MWCNTs from 0 to 3 wt% when the amount of POE was low (less than 5 w.%), while it slightly increased and then decreased when the amount of POE was high (more than wt%). In fact, it can be said that there is an interaction between the MWCNTs with tubular shape and POE in the case of the tensile strength of PLA. This result may be due to the saturation of the reinforcing action of the filler. As a result, lower values of POE as an impact modifier were useful for modifying the surface of MWCNTs and thus improving the interfacial interactions between the hydrophilic nanoparticles and hydrophobic polymer [47].

From Figure 6b it is observed that the tensile strength first increase and then decrease by increasing the carbon black content from 0 to 3 wt% in the presence of all POE concentrations. On the other hand, tensile strength considerably decreased and then slightly increased with increasing the amount of POE from 0 to 20 wt% when the amount of carbon black was 1 wt%. It seems that the excellent dispersion and distribution of carbon black nanoparticles at a concentration of 1 wt% in the binary PLA/POE matrix and the proper interaction between PLA, POE, and carbon black nanoparticles lead to this improvement in tensile strength. Therefore, it can be said that there is an interaction between the POE and 1 wt% carbon black in the case of tensile strength.

From Figure 6c (the tensile strength of hybrid nanocomposites) at the absence of POE, different trends are observed by the simultaneous addition of both nanofillers. In the way that the tensile strength of the matrix increase by increasing the MWCNTs content in lack of carbon black; while the trend of increase is not constant and it is changed by the presence of carbon black concentration and more altered to a decrease rate.

In general, the addition of MWCNTs in the presence of high content (up to 1 wt%) of carbon black is associated with a descending trend in the tensile strength. It can be concluded that because of high concentration (up to 2 wt%) and severe agglomeration, nanofillers are stuck together and by creating more stress concentration, have not been able to perform their main role of increasing strength. Therefore, it can be said that a negative interaction has existed

between the effect of MWCNTs and carbon black nanofillers on the tensile strength. Finally, Figure 6c demonstrates that the maximum values for tensile strength of hybrid nanocomposites are obtained by 2 wt% loading of carbon black.
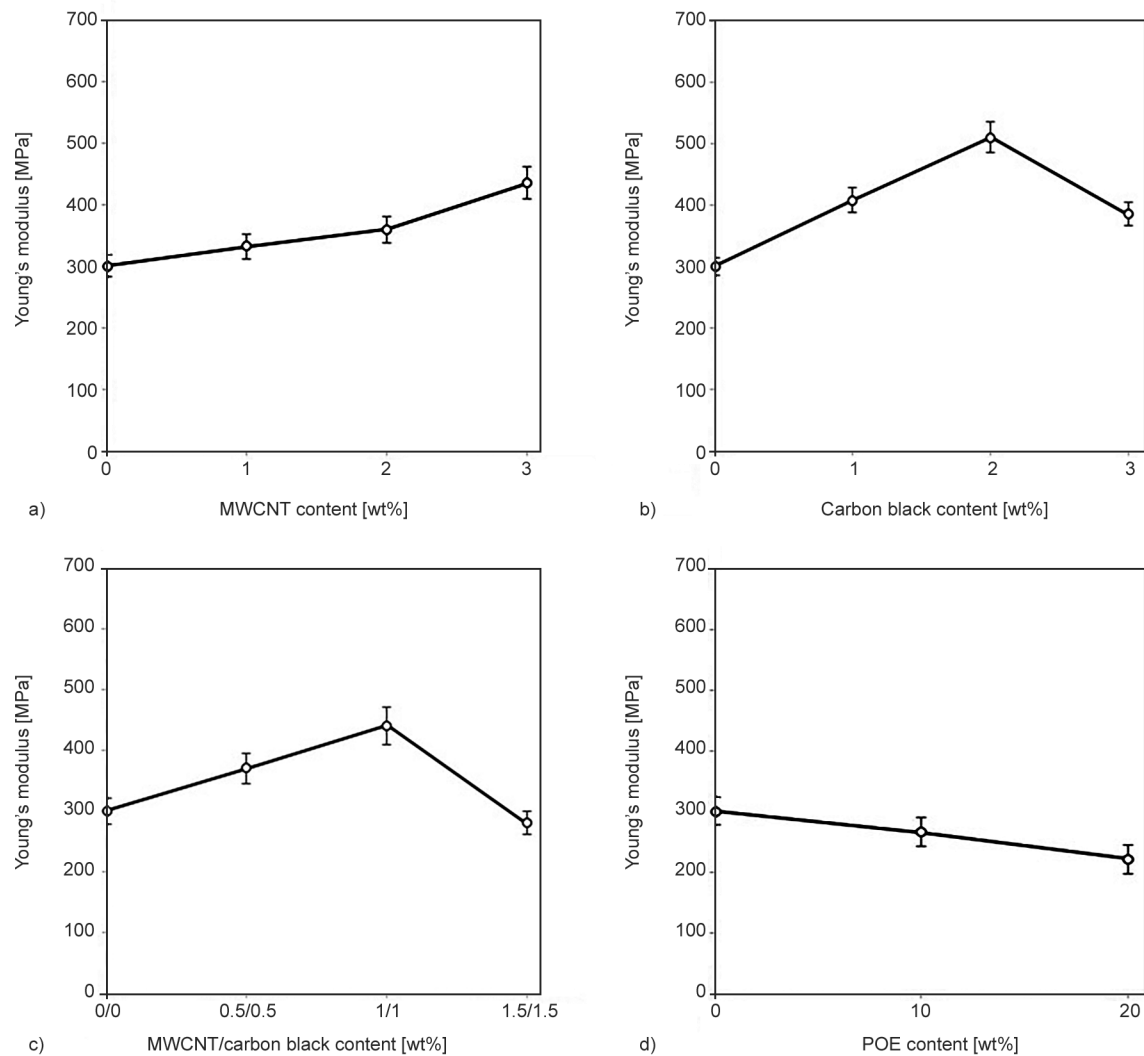
### 3.3.2. Young's modulus

The effect of POE and nanofillers on Young's modulus are presented in different parts of Figure 7. As demonstrates in Figure 7a, by increasing the MWCNTs content from low to high into the matrix, Young's modulus increases from 300 to 435 MPa continually. This ascending trend in Young's modulus proves that adding of MWCNTs up to 3 wt% loading deeply affects the stiffness of the matrix [48]. This improvement in Young's modulus is consistent with the outcomes of other researches that were carried out on PLA/MWCNTs compounds [49, 50].

Figure 7b indicates that Young's modulus of the PLA matrix was dramatically raised by increasing carbon black content up to 2 wt% from 300 to 506 MPa. Young's modulus of PLA improves with adding carbon black concentration since these spherical nanoparticles are stiffer than polymer matrix [46]. Liu *et al*. [45] reported that the addition of carbon black nanoparticles up to 5 wt% into the PLA matrix had increased its Young's modulus properly. From Figure 7b, a decrease in Young modulus is visible by adding 3 wt% carbon black into PLA because of their agglomeration as clearly depicts in Figure 3c. However, it should be noted that this decrease in Young's modulus is not severe, and it is still 37% higher than Young's modulus of pure PLA.

As shown in Figure 7c, Young's modulus of the PLA matrix improves from 300 to 403 MPa with increasing simultaneous MWCNTs and carbon black content up 1.5 wt% of each one in it. It can be explained that the simultaneous presence of both nanofillers in the case of hybrid nanocomposites has been able to create an increased trend in the stiffness of PLA. From the Figure 7a–7c, it is clear that the addition of individual nanofillers comparing to the simultaneous presence of them create more appropriate improvement in Young's modulus.

From Figure 7d, it can be observed a continual decrease in Young's modulus of PLA matrix from 300 to 221 MPa with increasing POE content. It is noted, when a polymer with high elasticity and low modulus at a high level is blended with a high modulus

**Figure 7.** Young's modulus of PLA *versus*: a) MWCNTs, b) carbon black, c) MWCNTs/carbon black, and d) POE.

polymer as a matrix, the resulting product will have a lower modulus compared to the pure matrix [11]. Forghani *et al*. [46] have been reported that the addition of POE in the PLA matrix reduces its Young's modulus.

Figure 8 illustrates the surfaces extracted from the FRBSs method for Young's modulus.

It is observed from Figure 8a that Young's modulus continually increased with increasing the amount of MWCNTs from 0 to 3 wt% in the presence of any amount of POE. The reason for the increase in Young's modulus can be attributed to the excellent sticking at the interface between the matrix and the filler. It is also observed that Young's modulus continually decreased with increasing the amount of POE from 0 to 20 wt% in the presence of any amount of MWCNTs. As can be seen from Figure 8b, it is clear that ascending and descending trends of Young's modulus by increasing carbon black nanoparticles in the presence

of the different amount of POE does not change. In fact, Figure 8a and 8b illustrate that there is no interaction between nanofillers and POE in the case of Young's modulus trends.

Also, from Figure 8c, it observes positive interaction between the effects of the simultaneous presence of fillers on Young's modulus. In fact, it can be said that by increasing carbon black concentrations from low to high levels in the presence of different loadings of MWCNTs and conversely, Young's modulus improves well. Also, Young's modulus decreased and then increased with increasing the amount of MWCNTs from 0 to 3 wt% when the amount of carbon black was 2 wt%. It seems that carbon black nanoparticles at 2 wt% concentration with good dispersion have been able to fill the gap between MWCNTs and the polymer matrix. Therefore, a synergy is created between fillers to increase Young's modulus of PLA matrix.
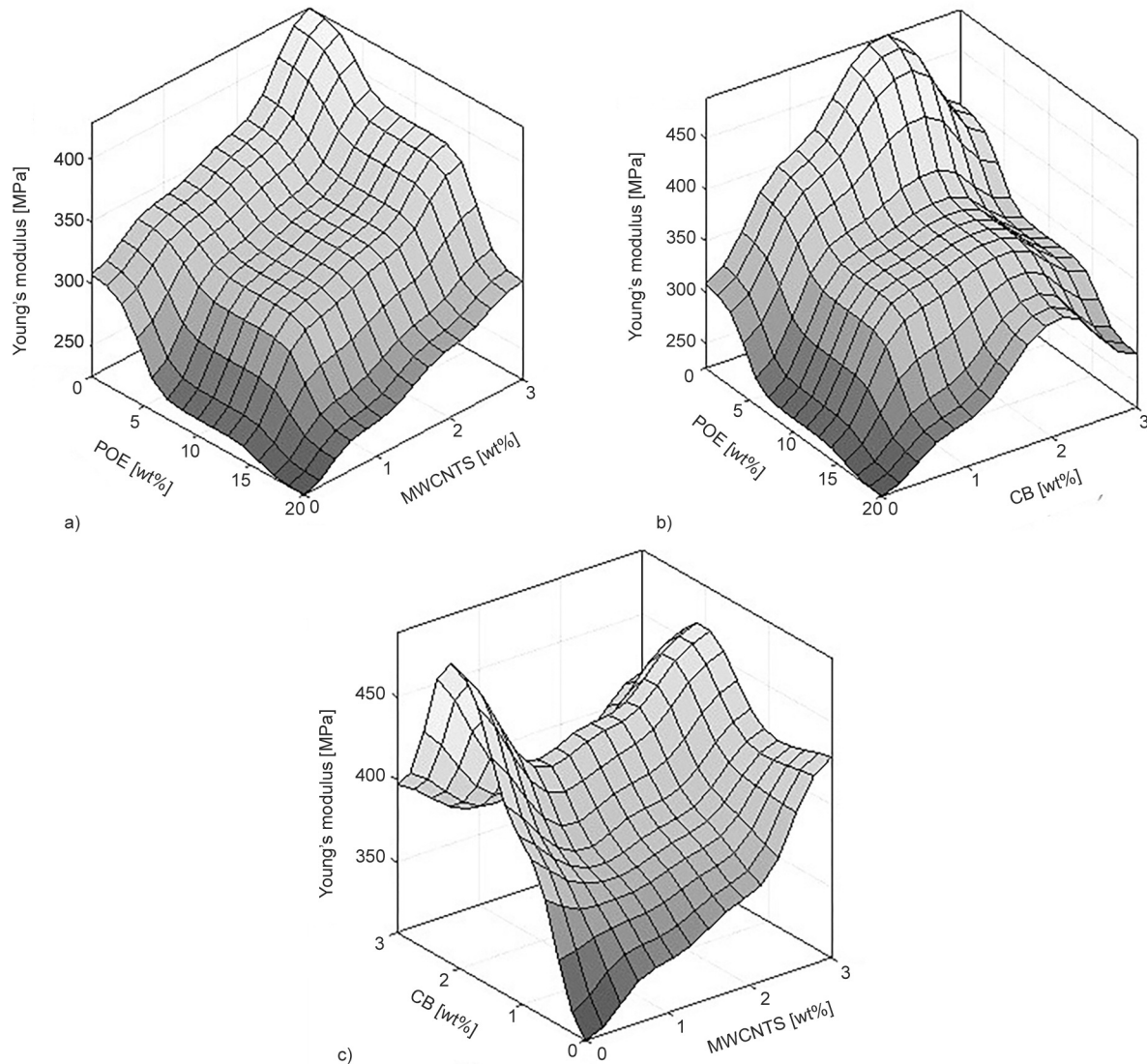
**Figure 8.** Surface plots for Young's modulus of PLA matrix versus: a) POE and MWCNTs, b) POE and carbon black, and c) MWCNTs and carbon black.
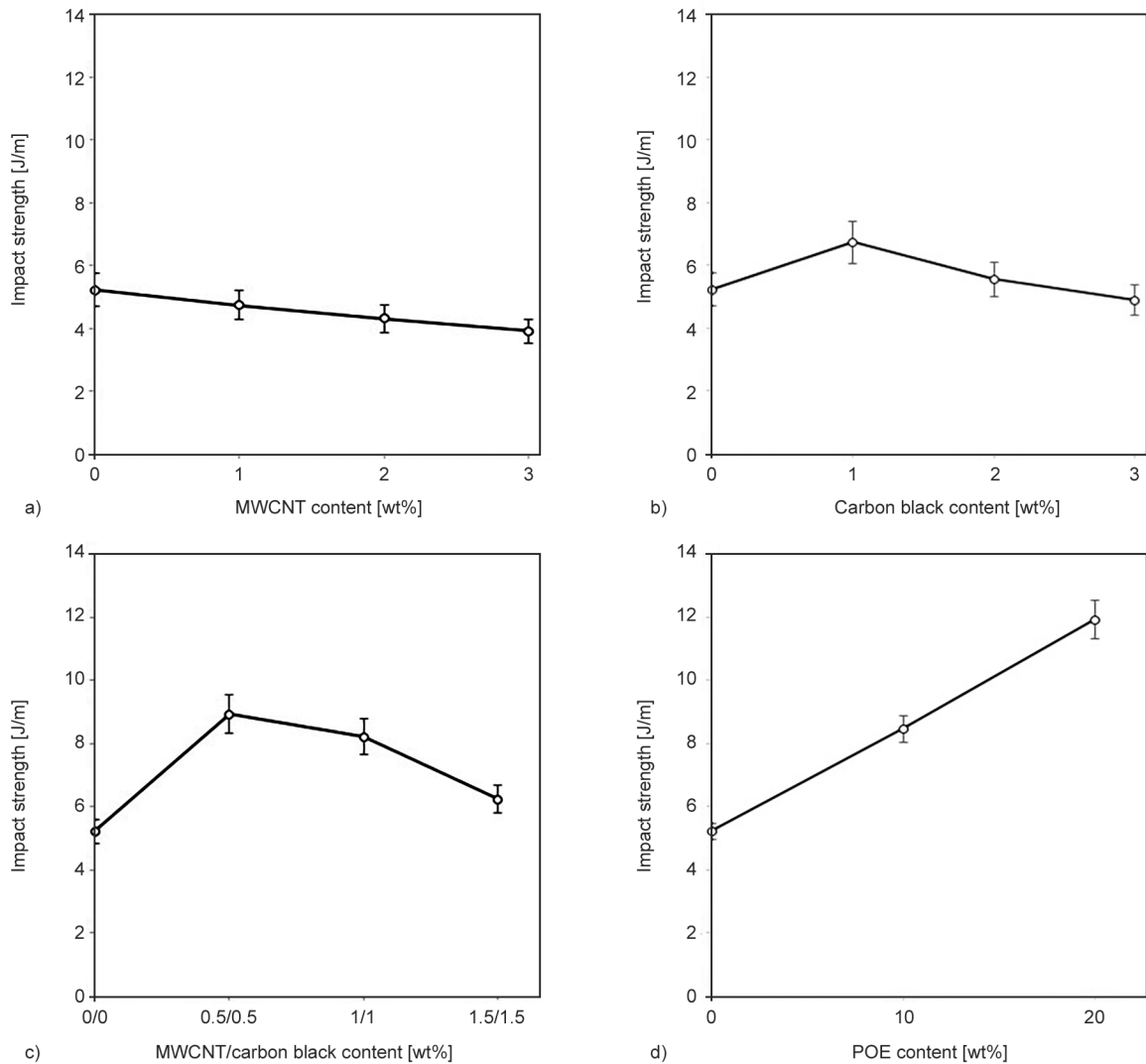
### 3.3.3. Impact strength

The Izod impact tests were carried out to finding the effect of POE, MWCNTs, and carbon black nanoparticles on the impact strength of the matrix, and obtained results are shown in different parts of Figure 9. According to Figure 9a, impact strength of the matrix decrease with increasing MWCNTs content from 0 to 3 wt% by 25%. In fact, the addition of MWCNTs to the matrix not only did not increase the impact strength but also increased its brittleness. Mat Desa *et al.* [50] also reported a descending trend in the case of impact strength for the PLA matrix modified by MWCNTs.

Figure 9b demonstrates that with the increase of carbon black content up to 1 wt%, the impact strength of the PLA matrix is improved by 29%. In addition, the impact strength of PLA decreases with an increase of

more than 1 wt% of carbon black content. Increasing the impact strength of PLA by the addition of 1 wt% content of carbon black is related to the holes created by them in the matrix (cavitation). These holes helped the PLA to absorb more energy during the impact tests and thus decreased its brittleness slightly. da Silva *et al.* [51] reported that the impact strength of the PLA matrix reduced by 9% with the addition of 15 wt% of carbon black into it, a slightly reducing.

As can be seen from Figure 9c, the impact strength of PLA/MWCNTs/carbon black nanocomposites has interestingly increased from 5.21 to 6.74 J/m. This increase, which was achieved by adding 1 wt% of each filler is not comparable to the impact strength of PLA/MWCNTs and PLA/carbon black compounds. It seems the simultaneous addition of MWCNTs and carbon black content up to 1 wt% of each one in the
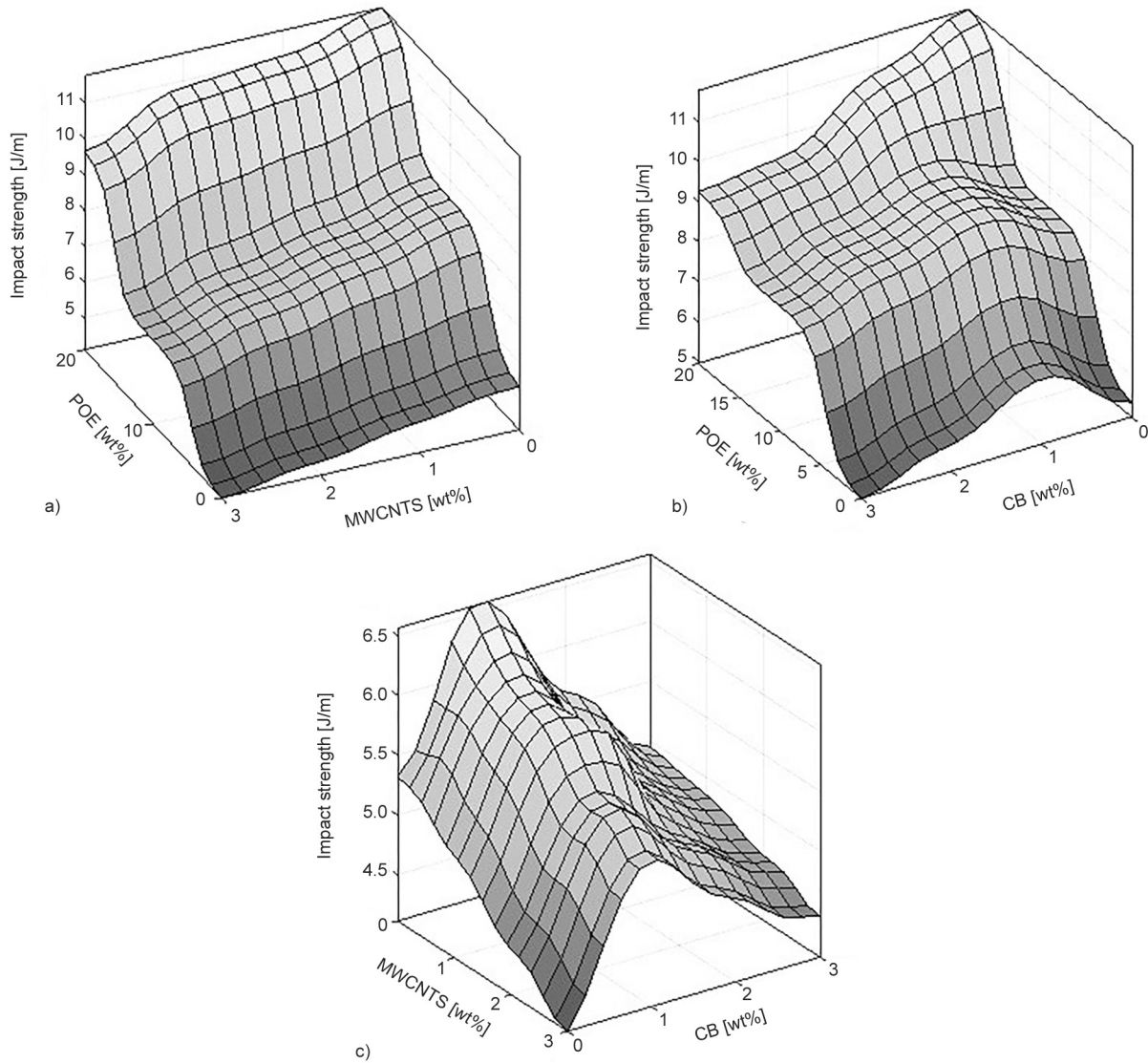
**Figure 9.** Impact strength of PLA *versus*: a) MWCNTs b) carbon black c) MWCNTs/carbon black, and d) POE.

PLA matrix creates a mechanism that dramatically reduces its brittleness. According to Figure 9d, adding POE from low to high levels dramatically increases the impact strength of PLA from 5.5 to 11.9 J/m, an increase 116%. It is obvious when high-energy absorbing polymers such as POE is blended with a brittle polymer such as PLA, the impact strength of the matrix increases.

Figure 10 illustrates the surfaces extracted from the FRBSs method for impact strength, as can be seen from Figure 10a, it is clear that the descending trend of impact strength for MWCNTs does not change in the presence of different contents of POE. This means that there is no interaction between MWCNTs and POE in the case of impact strength. From Figure 10b, it is observed that impact strength first increased and then decreased with increasing the amount of carbon black

nanoparticles from 0 to 3 wt% when the amount of POE altered from 0 to 15 wt%, while the addition of carbon black nanoparticles from low to high levels in the presence of more than 15 wt% of POE leads to a descending trends in impact strength. The reason for the decrease in the impact strength can be attributed to the poor sticking at the interface between carbon black nanoparticles and high amounts of POE in the PAL matrix.

According to Figure 10c, it can be said that by increasing MWCNTs contents from 0 to 3 wt% in the presence of different concentrations of carbon black and conversely, the trend of the impact strength of the PLA matrix does not alter. In addition, the maximum value for impact strength in the case of hybrid nanocomposites is achieved with the addition of 1 wt% carbon black in the lack of MWCNTs content, as clearly be seen in Figure 10c.

**Figure 10.** Surface plots for impact strength of PLA matrix versus: a) POE and MWCNTs, b) POE and carbon black, and c) MWCNTs and carbon black.

## 4. Conclusions

The main objective of this work was to use the FRBSs method for predicting and modeling POE, MWCNTs, and carbon black nanoparticles effects on the mechanical properties of the PLA matrix. A summary of the results is presented below:

1) Based on the tensile test results, the presence of carbon black nanoparticles and MWCNTs at the high-level contents led to improve Young's modulus by 68 and 45%, and tensile strength by 76 and 36%, respectively. Furthermore, the adding of POE to the matrix reduced Young's modulus from 300 to 221 MPa.

2) Based on the results of the impact tests, the addition of POE to PLA resulted in a proper increase

in impact strength by 128%. In addition, the simultaneous presence of 1 wt% loading of each filler led to an increase in impact strength by 30%. Also, adding carbon black nanoparticles only at 1 wt% content was able to create about 29% increase in impact strength.

3) The models presented for mechanical properties in terms of input variables using the FRBSs method and Microsoft Excel Office Software have a value of $R^2$ close to 1, and their standard error value is approximately near to 3. Furthermore, the surfaces extracted from the FRBSs method showed that there is an interaction between the carbon black nanoparticles and the MWCNTs in the case of mechanical properties.

## References

[1] Gu L., Qiu J., YaoY., Sakai E., Yang L.: Functionalized MWCNTs modified flame retardant PLA nanocomposites and cold rolling process for improving mechanical properties. Composite Science and Technology, **161**, 39–49 (2018).
https://doi.org/10.1016/j.compscitech.2018.03.033

[2] Zare Y., Garmabi H., Rhee K. Y.: Structural and phase separation characterization of poly(lactic acid)/poly(ethylene oxide)/carbon nanotube nanocomposites by rheological examinations. Composites Part B: Engineering, **144**, 1–10 (2018).
https://doi.org/10.1016/j.compositesb.2018.02.024

[3] Chakraborty G., Valapa R. B., Pugazhenthi G., Katiyar V.: Investigating the properties of poly(lactic acid)/exfoliated graphene based nanocomposites fabricated by versatile coating approach. International Journal of Biological Macromolecules, **113**, 1080–1091 (2018).
https://doi.org/10.1016/j.ijbiomac.2018.03.037

[4] Hamad K., Kaseem M., Deri F.: Rheological and mechanical properties of poly(lactic acid)/polystyrene polymer blend. Polymer Bulletin, **65**, 509–519 (2010).
https://doi.org/10.1007/s00289-010-0354-2

[5] Ishida S., Nagasaki R., Chino K., Dong T., Inoue Y.: Toughening of poly(L-lactide) by melt blending with rubbers. Journal of Applied Polymer Science, **113**, 558–566 (2009).
https://doi.org/10.1002/app.30134

[6] Bourmaud A., Pimbert S.: Investigations on mechanical properties of poly(propylene) and poly(lactic acid) reinforced by miscanthus fibers. Composites Part A: Applied Science and Manufacturing, **39**, 1444–1454 (2008).
https://doi.org/10.1016/j.compositesa.2008.05.023

[7] Lin S., Guo W., Chen C., Ma J., Wang B.: Mechanical properties and morphology of biodegradable poly(lactic acid)/poly(butylene adipate-*co*-terephthalate) blends compatibilized by transesterification. Materials and Design **36**, 604–608 (2012).
https://doi.org/10.1016/j.matdes.2011.11.036

[8] Anderson K. S., Hillmyer M. A.: The influence of block copolymer microstructure on the toughness of compatibilized polylactide/polyethylene blends. Polymer, **45**, 8809–8823 (2004).
https://doi.org/10.1016/j.polymer.2004.10.047

[9] Wang S., Pang S., Pan L., Xu N., Huang H., Li T.: Compatibilization of poly(lactic acid)/ethylene-propylene-diene rubber blends by using organic montmorillonite as a compatibilizer. Journal of Applied Polymer Science, 133, 1–10 (2016).
https://doi.org/10.1002/app.44192

[10] Yeh J-T., Tsou C-H., Huang C-Y., Chen K-N., Wu C-S., Chai W-L.: Compatible and crystallization properties of poly(lactic acid)/poly(butylene adipate-*co*-terephthalate) blends. Journal of Applied Polymer Science, **116**, 680–687 (2009).
https://doi.org/10.1002/app.30907

[11] Zhou J. T., Yao Z. J., Zhou J. J.: Crystallinity and mechanical properties of PLA/POE blends. Advanced Materials Research, **335**, 886–890 (2011).
https://doi.org/10.4028/www.scientific.net/AMR.335-336.886

[12] Zhang H-C., Kang B-H., Chen L-S., Lu X.: Enhancing toughness of poly(lactic acid)/thermoplastic polyurethane blends *via* increasing interface compatibility by polyurethane elastomer prepolymer and its toughening mechanism. Polymer Testing, **87**, 106521 (2020).
https://doi.org/10.1016/j.polymertesting.2020.106521

[13] Balakrishnan H., Hassan A., Imran M., Wahit M. U.: Toughening of polylactic acid nanocomposites: A short review. Polymer Plastic Technology Engineering, **51**, 175–192 (2012).
https://doi.org/10.1080/03602559.2011.618329

[14] Yang L., Chen H., Jia S., Lu X., Huang J., Yu X., Ye K., He G., Qu J.: Influences of ethylene–butylacrylate–glycidyl methacrylate on morphology and mechanical properties of poly(butylene terephthalate)/polyolefin elastomer blends. Journal of Applied Polymer Science **131**, 40660 (2014).
https://doi.org/10.1002/app.40660

[15] Guo Z., Fang Z., Tong L.: Application of percolation model on the brittle to ductile transition for polystyrene and polyolefin elastomer blends. Express Polymer Letters, **1**, 37–43 (2007).
https://doi.org/10.3144/expresspolymlett.2007.8

[16] Liu G., Qiu G.: Study on the mechanical and morphological properties of toughened polypropylene blends for automobile bumpers. Polymer Bulletin, **70**, 849–857 (2012).
https://doi.org/10.1007/s00289-012-0880-1

[17] da Silva K. I. M., Fernandes J. A., Kohlrausch E. C., Dupont J., Santos M. J. L., Gil M. P.: Structural stability of photodegradable poly(L-lactic acid)/PE/$TiO_2$ nanocomposites through $TiO_2$ nanospheres and $TiO_2$ nanotubes incorporation. Polymer Bulletin, **71**, 1205–1217 (2014).
https://doi.org/10.1007/s00289-014-1119-0

[18] Chieng B. W., Ibrahim N. A., Yunus W. M., Hussein M. Z.: Poly(lactic acid)/poly(ethylene glycol) polymer nanocomposites: Effects of graphene nanoplatelets. Polymer, **6**, 93–104 (2014).
https://doi.org/10.3390/polym6010093

[19] Yang W., Tawiah B., Yu C., Qian Y-F., Wang L-L., Yuen A. C-Y., Zhu S-E., Hu E-Z., Chen T. B-Y., Yu B., Lu H-D., Yeoh G. H., Wang X., Song L., Hu Y.: Manufacturing, mechanical and flame retardant properties of poly(lactic acid) biocomposites based on calcium magnesium phytate and carbon nanotubes. Composites Part A: Applied Science and Manufacturing, **110**, 227–236 (2018).
https://doi.org/10.1016/j.compositesa.2018.04.027

[20] Wang L., Qiu J., Sakai E., Wei X.: The relationship between microstructure and mechanical properties of carbon nanotubes/polylactic acid nanocomposites prepared by twin-screw extrusion. Composites Part A: Applied Science and Manufacturing, **89**, 18–25 (2016).
https://doi.org/10.1016/j.compositesa.2015.12.016

[21] Scaffaro R., Lopresti F.: Properties-morphology relationships in electrospun mats based on polylactic acid and graphene nanoplatelets. Composites Part A: Applied Science and Manufacturing, **108**, 23–29 (2018).
https://doi.org/10.1016/j.compositesa.2018.02.026

[22] Pinto R. M., Cabral J., Tanaka D. A. P., Mendes A. M., Magalhães F. D.: Effect of incorporation of graphene oxide and graphene nanoplatelets on mechanical and gas permeability properties of poly(lactic acid) films. Polymer International, **62**, 33–40 (2013).
https://doi.org/10.1002/pi.4290

[23] Wang N., Zhang X., Ma X., Fang J.: Influence of carbon black on the properties of plasticized poly(lactic acid) composites. Polymer Degradation and Stability, **93**, 1044–1052 (2008).
https://doi.org/10.1016/j.polymdegradstab.2008.03.023

[24] Costa R. G. F., Brichi G. S., Ribeiro C., Mattoso L. H. C.: Nanocomposite fibers of poly(lactic acid)/titanium dioxide prepared by solution blow spinning. Polymer Bulletin, **73**, 2973–2985 (2016).
https://doi.org/10.1007/s00289-016-1635-1

[25] Najafi N., Heuzey M. C., Carreau P. J.: Polylactide (PLA)-clay nanocomposites prepared by melt compounding in the presence of a chain extender. Composites Science and Technology, **72**, 608–615 (2012).
https://doi.org/10.1016/j.compscitech.2012.01.005

[26] Lai S-M., Hsieh Y-T.: Preparation and properties of polylactic acid (PLA)/silica nanocomposites. Journal of Macromolecular Science Part B: Physics, **55**, 211–228 (2016).
https://doi.org/10.1080/00222348.2016.1138179

[27] Al-Saleh M. H.: Electrical and mechanical properties of graphene/carbon nanotube hybrid nanocomposites. Synthetic Metals, **219**, 41–46 (2015).
https://doi.org/10.1016/j.synthmet.2015.06.023

[28] Ramesh P., Durga Prasad B., Narayana K. L.: Effect of MMT clay on mechanical, thermal and barrier properties of treated aloevera fiber/PLA-hybrid biocomposites. Silicon, **12**, 1751–1760 (2020).
https://doi.org/10.1007/s12633-019-00275-6

[29] Palawat N., Chaiwutthinan P., Limpanart S., Larpkasemsuk A., Boonmahitthisud A.: Hybrid nanocomposites of poly(lactic acid)/thermoplastic polyurethane with nanosilica/montmorillonite. Materials Science Forum, **947**, 77–81 (2019).
https://doi.org/10.4028/www.scientific.net/MSF.947.77

[30] Tanyildizi H.: Fuzzy logic model for prediction of mechanical properties of lightweight concrete exposed to high temperature. Materials Design, **30**, 2205–2210 (2009).
https://doi.org/10.1016/j.matdes.2008.08.030

[31] Daneshpayeh S., Tarighat A., Ashenai Ghasemi F., Bagheri M. S.: A fuzzy logic model for prediction of tensile properties of epoxy/glass fiber/silica nanocomposites. Journal of Elastomers and Plastics, **50**, 491–500 (2018).
https://doi.org/10.1177%2F0095244317733768

[32] Rajmohan T., Palanikumar K., Prakash S.: Grey-fuzzy algorithm to optimise machining parameters in drilling of hybrid metal matrix composites. Composites Part B: Engineering, **50**, 297–308 (2013).
https://doi.org/10.1016/j.compositesb.2013.02.030

[33] Lea R. N.: Applications of fuzzy sets to rule-based expert system development. Telematics and Informatics, **6**, 403–406 (1989).
https://doi.org/10.1016/S0736-5853(89)80030-9

[34] Perfilieva I.: Analytical theory of fuzzy IF-THEN rules with compositional rule of inference. in 'Fuzzy logic' (eds.: Wang P. P., Ruan D., Kerre E. E.) Springer, Berlin, Vol 215, 174–191 (2007).
https://doi.org/10.1007/978-3-540-71258-9_9

[35] Egaji O. A., Griffiths A., Hasan M. S., Yu H-N.: A comparison of Mamdani and Sugeno fuzzy based packet scheduler for MANET with a realistic wireless propagation model. International Journal of Automation and Computing, **12**, 1–13 (2015).
https://doi.org/10.1007/s11633-014-0861-y

[36] Mondal S., Khastgir D.: Elastomer reinforcement by graphene nanoplatelets and synergistic improvements of electrical and mechanical properties of composites by hybrid nano fillers of graphene-carbon black & graphene-MWCNT. Composites Part A: Applied Science and Manufacturing, **102**, 154–165 (2017).
https://doi.org/10.1016/j.compositesa.2017.08.003

[37] McCullen S. D., Stano K. L., Stevens D. R., Roberts W. A., Monteiro-Riviere N. A., Clarke L. I., Gorga R. E.: Development, optimization, and characterization of electrospun poly(lactic acid) nanofibers containing multiwalled carbon nanotubes. Journal of Applied Polymer Science, **105**, 1668–1678 (2007).
https://doi.org/10.1002/app.26288

[38] Wu S.: A generalized criterion for rubber toughening: The critical matrix ligament thickness. Journal of Applied Polymer Science, **35**, 549–561 (1988).
https://doi.org/10.1002/app.1988.070350220

[39] Ren F., Li Z., Xu L., Sun Z., Ren P., Yan D., Li Z.: Large-scale preparation of segregated PLA/carbon nanotube composite with high efficient electromagnetic interference shielding and favourable mechanical properties. Composites Part B: Engineering, **155**, 405–413 (2018).
https://doi.org/10.1016/j.compositesb.2018.09.030

[40] Ismail H., Ramly A. F., Othman N.: The effect of carbon black/multiwall carbon nanotube hybrid fillers on the properties of natural rubber nanocomposites. Polymer-Plastics Technology and Engineering, **50**, 660–666 (2011).
https://doi.org/10.1080/03602559.2010.551380

[41] Wang X., Jiang B., Liu J. S.: Generalized R-squared for detecting dependence. Biometrika, **104**, 129–139 (2017).
https://doi.org/10.1093/biomet/asw071

[42] Lewis-Beck M. S., Skalaban A.: The R-squared: Some straight talk. Political Analysis, **2**, 153–171 (1990).
https://doi.org/10.1093/pan/2.1.153

[43] Mbatha C. N., Gustafsson M. A.: The standard error of regressions: A note on new evidence of significance misuse. Agrekon, **52**, 28–39 (2013).
https://doi.org/10.1080/03031853.2013.778463

[44] Kuan C-F., Kuan H-C., Ma C-C. M., Chen C-H.: Mechanical and electrical properties of multi-wall carbon nanotube/poly(lactic acid) composites. Journal of Physics and Chemistry of Solids, **69**, 1395–1398 (2008).
https://doi.org/10.1016/j.jpcs.2007.10.060

[45] Liu H., Bai D., Bai H., Zhang Q., Fu Q.: Manipulating the filler network structure and properties of polylactide/carbon black nanocomposites with the aid of stereocomplex crystallites. Journal of Physics and Chemistry C, **122**, 4232–4240 (2018).
https://doi.org/10.1021/acs.jpcc.8b00417

[46] Forghani E., Azizi H., Karabi M., Ghasemi I.: Compatibility, morphology and mechanical properties of polylactic acid/polyolefin elastomer foams. Journal of Cellular Plastics, **54**, 235–255 (2018).
https://doi.org/10.1177%2F0021955X16681450

[47] Ashenai Ghasemi F., Daneshpayeh S., Ghasemi I., Ayaz M.: An investigation on the Young's modulus and impact strength of nanocomposites based on polypropylene/linear low-density polyethylene/titan dioxide (PP/LLDPE/$TiO_2$) using response surface methodology. Polymer Bulletin, **73**, 1741–1760 (2016).
https://doi.org/10.1007/s00289-015-1574-2

[48] Kanbur Y., Küçükyavuz Z.: Electrical and mechanical properties of polypropylene/carbon black composites. Journal of Reinforced Plastics and Composites, **28**, 2251–2260 (2009).
https://doi.org/10.1177%2F0731684408092378

[49] Moon S-I., Jin F., Lee C-J., Tsutsumi S., Hyon S-H.: Novel carbon nanotube/poly(L-lactic acid) nanocomposites; Their modulus, thermal stability, and electrical conductivity. Macromolecular Symposia, **224**, 287–296 (2005).
https://doi.org/10.1002/masy.200550625

[50] Mat Desa M. S. Z., Hassan A., Arsad A., Mohammad N. N. B.: Mechanical properties of poly(lactic acid)/multiwalled carbon nanotubes nanocomposites. Material Research Innovations, **18**, 14–17 (2014).
https://doi.org/10.1179/1432891714Z.000000000924

[51] da Silva T. F., Menezes F., Montagna L. S., Lemes P., Passador F. R.: Preparation and characterization of antistatic packaging for electronic components based on poly(lactic acid)/carbon black composites. Journal of Applied Polymer Science, **136**, 47273 (2019).
https://doi.org/10.1002/app.47273